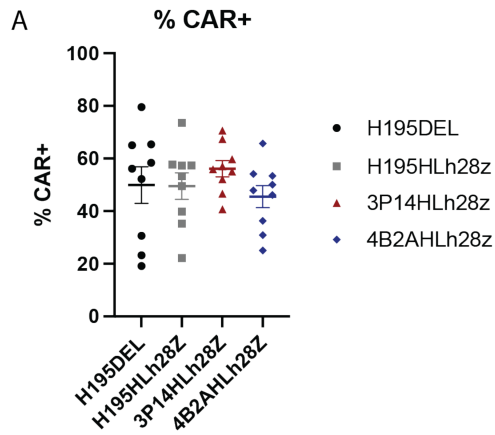


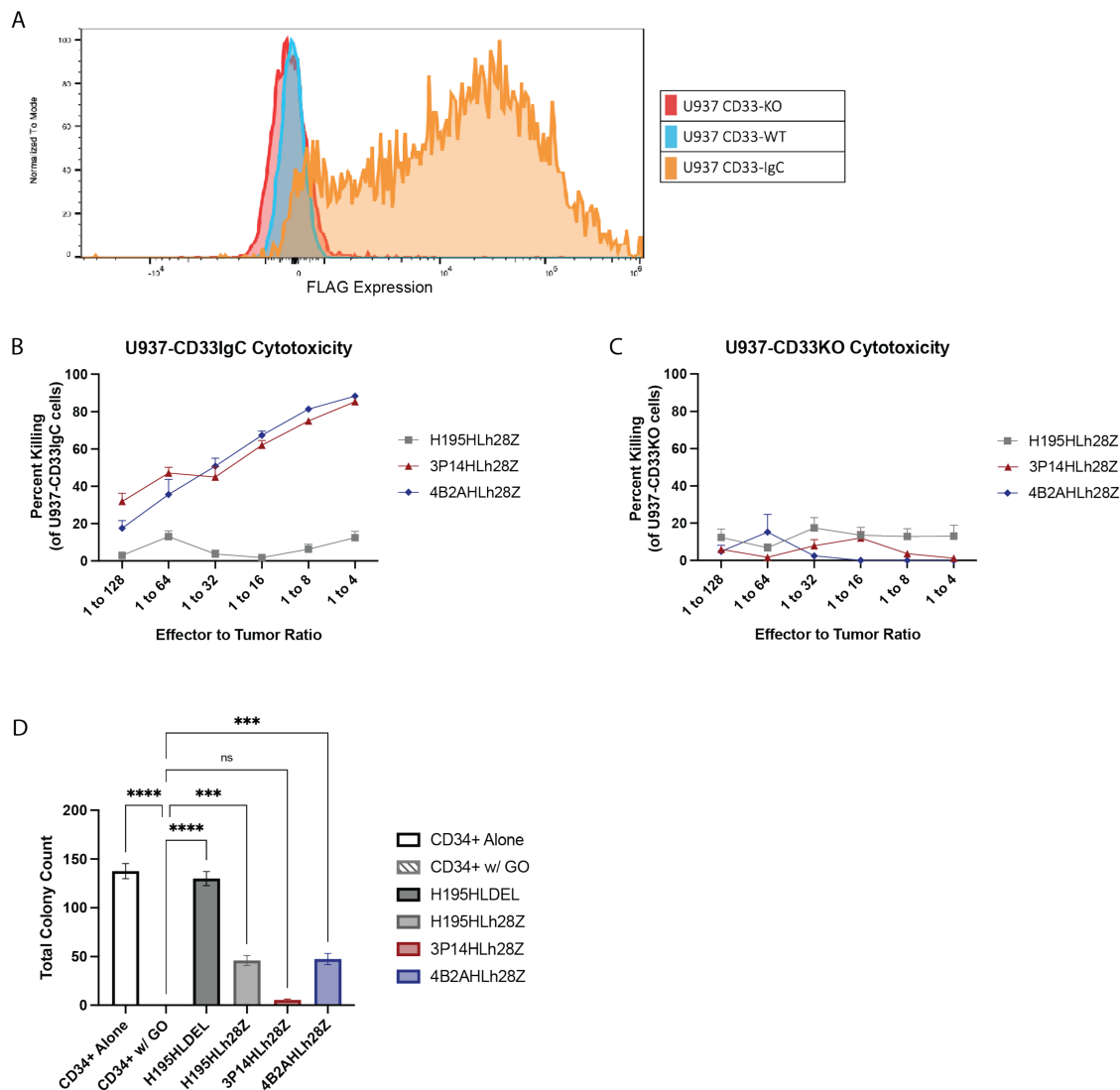
Supplemental Figure 1. Selection of a membrane-proximal CD33-IgC targeting scFv

(A) Flow cytometry histograms of CD33 expression on 3T3-wildtype and 3T3-CD33 cells detected with fluorescently labeled CD33-specific antibody. (B) Flow cytometry histograms of CD33 expression on U937-wildtype and U937-CD33-knockout cells detected with fluorescently labeled CD33-specific antibody. (C) Quantification of hybridoma-derived monoclonal antibody cross-reactivity as measured by His tag binding. (D) Quantification of hybridoma-derived monoclonal antibody binding kinetics to CD33 in solution. (E) Quantification of EC_{50} of lead

hybridoma-derived monoclonal antibodies on overexpressing (3T3) and AML cell line (U937).
(F) Quantification of epitope binning of selected hybridoma-derived monoclonal antibodies.

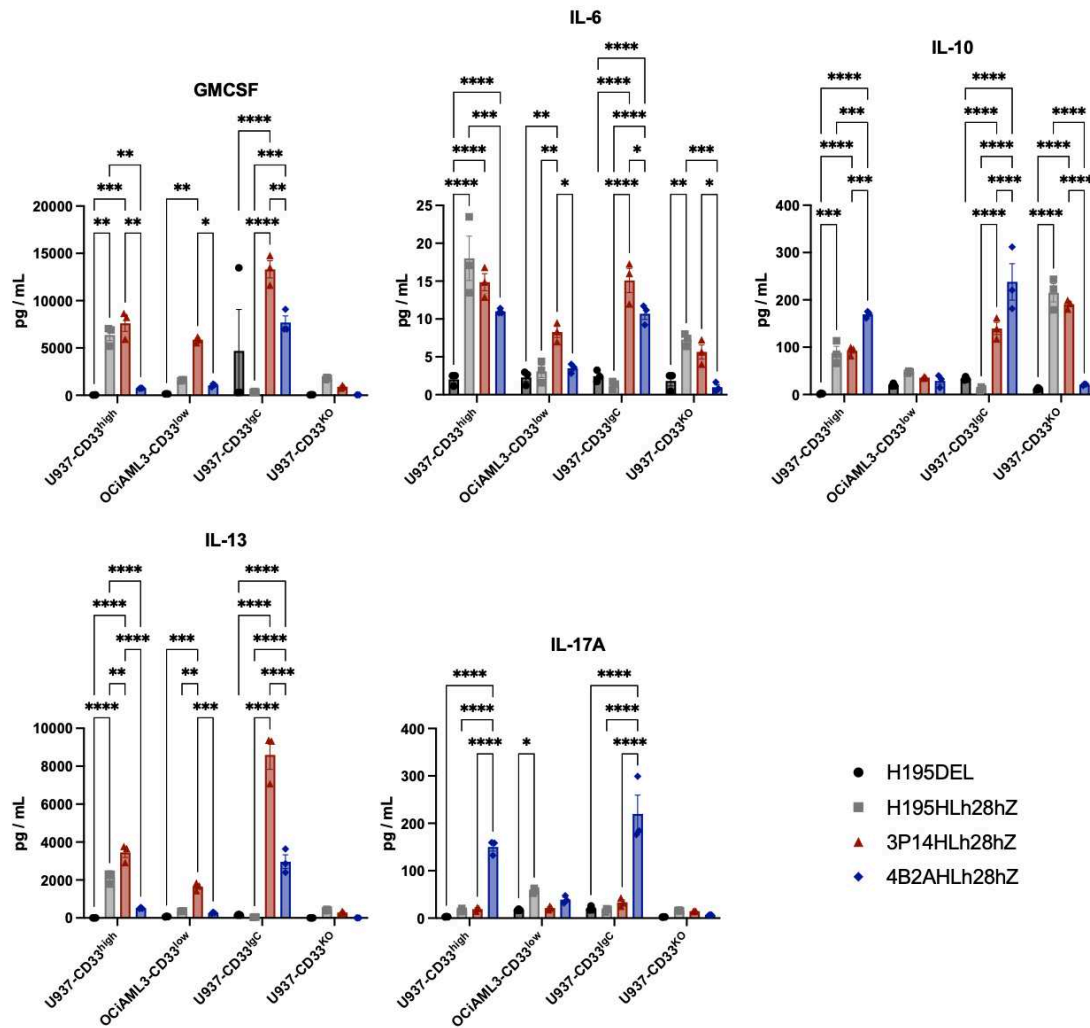


Supplemental Figure 2. Transduction efficiencies of CAR T cells used for in vitro analysis
(A) Dot plot showing CAR expression following human T cell transduction with 4 CAR constructs as detected with fluorescently labeled cetuximab by flow cytometry (n=9 independent biological donors).

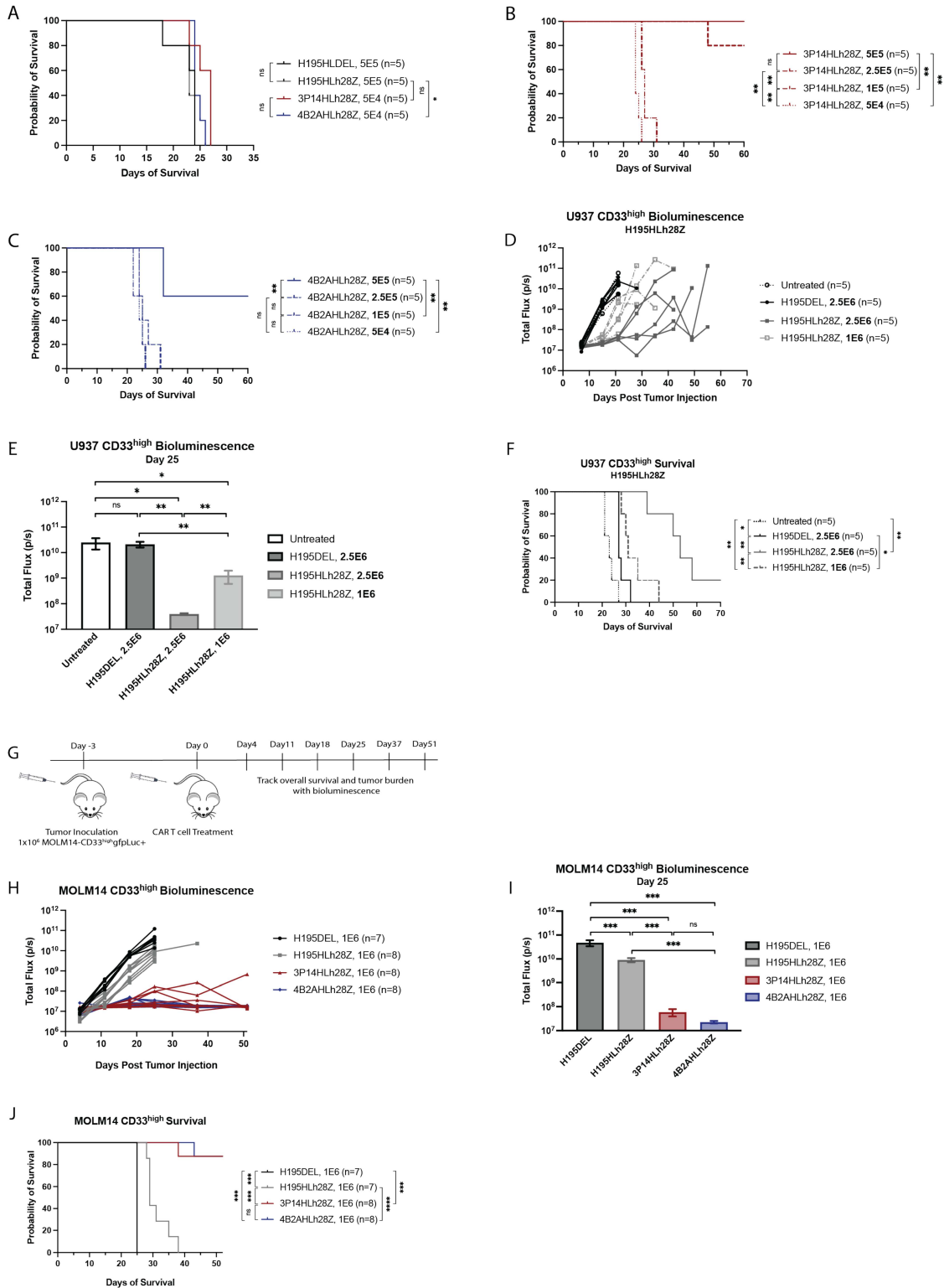


Supplemental Figure 3. Specificity of membrane-proximal targeting CAR T cells

(A) Flow cytometry histograms depicting FLAG expression on transduced U937-CD33^{IgC} tumor cells. (B) 24-hour D-luciferin assay demonstrating lysis of U937-CD33^{IgC} tumor cells. Data representative of two independent experiments. (C) 24-hour D-luciferin assay demonstrating lysis of U937-CD33^{KO} tumor cells. Data representative of two independent experiments. (D) Quantification of total colonies produced using a colony-forming unit (CFU) assay to measure hematopoietic killing, where total colony count is a composite of BFU-E, GEMM-CFU, and GM-CFU ($n = 9$; ****, $P < 0.0001$; ***, $P < 0.001$ by ordinary one-way ANOVA; ns, non-significant). Data are a mean \pm SEM of three biological replicates conducted in three independent experiments.



Supplemental Figure 4. 24-hour cytokine secretion profile of CAR-T cells when co-cultured with U937-CD33^{high}, OCiAML3-CD33^{low}, U937-CD33^{IgC}, and U937-CD33^{KO} tumor as detected by human 12-plex Luminex panel ($n = 3$; ****, $P < 0.0001$; ***, $P < 0.001$; **, $P < 0.01$; *, $P < 0.05$ by two-way ANOVA). Data are a mean \pm SEM of 3 biological replicates conducted in 3 independent experiments.



Supplemental Figure 5. Membrane-proximal CD33-targeting CAR T cells provide enhanced survival in xenograft mouse model (A) Survival of NCG mice bearing U937-CD33^{high} tumors and treated with 5.0×10^4 CAR T cells ($n = 5$; *, $P < 0.05$). P values for survival determined by log-rank Mantel-Cox test, with 95% confidence interval. (B) Survival of NCG mice bearing U937-CD33^{high} tumors and treated with titrated doses of 3P14HLh28hZ CAR T cells ($n = 5$; **, $P < 0.01$). P values for survival determined by log-rank Mantel-Cox test, with 95% confidence interval. (C) Survival of NCG mice bearing U937-CD33^{high} tumors and treated with titrated doses of 4B2AHLh28hZ CAR T cells ($n = 5$; **, $P < 0.01$). P values for survival determined by log-rank Mantel-Cox test, with 95% confidence interval. (D) Bioluminescence over time of U937-CD33^{high} in tumor-bearing NCG mice treated with higher doses of CAR T cells. (E) Day 25 bioluminescent total body flux of U937-CD33^{high} tumor-bearing NCG mice treated with higher doses of CAR T cells. (F) Survival of NCG mice bearing U937-CD33^{high} tumors and treated with higher doses of CAR T cells ($n = 5$, **, $P < 0.01$; *, $P < 0.05$). P values for survival determined by log-rank Mantel-Cox test, with 95% confidence interval. (G) Schematic diagram of *in vivo* experimental setup. NCG mice were inoculated with MOLM14-CD33^{high} tumor and subsequently treated with CAR T cells. (H) Bioluminescence over time of MOLM14-CD33^{high} in tumor-bearing NCG mice treated with 1.0×10^6 CAR T cells. (I) Day 25 bioluminescent total body flux of MOLM14-CD33^{high} tumor-bearing NCG mice treated with 1.0×10^6 CAR T cells. (J) Survival of NCG mice bearing MOLM14-CD33^{high} tumors and treated with 1.0×10^6 CAR T cells ($n = 7$ or 8 , ****, $P < 0.0001$; ***, $P < 0.001$; ns, non-significant). P values for survival determined by log-rank Mantel-Cox test, with 95% confidence interval.

Supplemental Table 1. Flow cytometry antibodies.

Specificity	Clone	Fluorophore
CD69	FN50	BV750
CD183	G025H7	BV650
CD152	L3D10	PE-Cy7
CD244	C1.7	APC
CD357	108-17	APC-Fire 750
CD197	2-L1-A	BUV395
CD45RO	UCHL1	SB702
CD3	UCHT1	BUV496
TCR alpha/beta	IP26	Brilliant Violet 510
TCR gamma/delta	B1	Alexa Fluor 532
CD223	11C3C65	PerCP-Cy5.5
CD194	MM0064-9G12	DyLight 550
CD45RA	HI100	Alexa Fluor 594
EGFR		PE
CD186	13B 1E5	FITC
CD272	J168-540	PE-CF594
CD134	L106	BV711
CD278	DX29	BV421
CD4	RPA-T4	APC-Cy7
CD279	EH12.2H7	BV785
TIGIT	MBSA43	PerCP-eF710
CD137	4B4-1	BUV661
CD127	A019D5	PE-Cy5
CD28	L293	BB700
CD45	HI30	APC Cy7
CD45 (mouse)	30-F11	Alexa Fluor 700
CD8	SK1	Alexa Fluor 700
CD366	7D3	PE-Cy5.5
CD103	BER-ACT8	BV605
CD25	2A3	BUV563
CD57	NK-1	eF450
CD95	DX29	BV480
CD27	O323	Alexa Fluor 647
HLA-DR	G46-6	APC-R700
CD33	WM53	PE-Cy7, BV711
CD62L	DREG-56	PE
CD2	TS1/8	FITC
CD371	50C1	APC
CD123	S18016F	PE-Cy7
TIM3	F38-2E2	BV510
Myc tag	9B11	PE, Alexa Fluor 647, Alexa Fluor 488

Supplemental Table 2. CD33 antigen density.

Cell Line	CD33 Antigen Density
MOLM14	10114.3
U937	6598.0
U937 CD33-KO	0
U937 CD33-IgC	94.4
OCiAML3	928.4
AML60B	8590.7

Supplemental Table 3. Characterization of patient-derived xenograft

	Age	Disease Status	Molecular Aberrations	Cytogenetics
AML60B	40	Relapsed/Refractory	KMT2A-MLLT3 fusion, PDGFRA loss, GSK3B, GATA2	MLL (11q23)

Supplemental Methods

In vitro colony forming unit assay

PBMCs were isolated from healthy umbilical cord blood units (New York Blood Center). Following red blood cell lysis with ACK Lysing Buffer (Lonza), CD34⁺ stem cells were isolated and subsequently expanded in Serum-Free Expansion Medium (SFEM) II and 1.0 μ M UM171 (StemCell Technologies). Expanded CD34⁺ progenitors and CAR T cells were co-cultured at 1:1 cell ratio for approximately 48 hours. Treated human CD34⁺ progenitors were seeded at a density of 3,333 cells/condition into cytokine-supplemented methylcellulose medium (MethoCult H4435; STEMCELL Technologies) on 6-well plates. Each condition was cultured in triplicate. Colonies were propagated in culture and scored at day 10 and counts were averaged across replicates.

Epitope binning

For epitope binning, human CD33-His was captured by an anti-penta-His biosensor. A 3x3 matrix with 3P14, 4B2A, and H195 was tested. A buffer-only reference biosensor was used to determine the overall capture level for each antibody. After pre-binding the antibodies at saturation levels, the biosensors were dipped into antibody solutions to assess competition.

Evaluation of CD33 surface densities

The surface densities of CD33 molecules on the cancer cells were examined by standardized flow cytometry using a commercial quantitative analysis kit, QIFIKIT® (Agilent) following the user manual provided by the manufacturer of the kit. Briefly, we set up and optimized the voltages for forward-scattering (FSC), side-scattering (SSC), and BL1 fluorescence channel (for

fluorescein isothiocyanate, FITC) in Attune NxT Flow Cytometer (Invitrogen) using the set-up beads (QIFIKIT®). Next, following standard staining and washing procedures, we stained the calibration beads (QIFIKIT®), a combination of 5 populations of beads bearing different known numbers of mouse antibodies on their surfaces, with FITC-conjugated goat anti-mouse immunoglobulin F(ab')₂ fragment. Then, using flow cytometry, the mean fluorescence intensities (MFIs) of the calibration beads of known surface densities, represented by antigen binding capacity (ABC) values, were recorded, from which a standard curve between the MFI and ABC values was constructed.